

X-ray diffraction analysis of residual stresses in surfaces subjected to cutting operations

Ing. Kamil Kolařík, Ph.D.¹, prof. Ing. Nikolaj Ganev, CSc.², Ing. Zdenek Pala¹,
Doc. Ing. Jan Jersák, CSc.²

¹Department of Solid State Engineering, Faculty of Nuclear Sciences and Physical Engineering, Czech Technical University in Prague, Trojanova 13, 120 00 Prague 2, Czech Republic

²Department of Machining and Assembly, Faculty of Mechanical Engineering, TUL of Liberec, Studentská 2, 461 17 Liberec 1, Czech Republic

Corresponding author, e-mail address: kamil.kolarik@email.cz

Two examples of X-ray diffraction (XRD) tensometry performed in XRD laboratory of Faculty of Nuclear Sciences and Physical Engineering of the Czech TU in Prague are specified in the contribution. They both deal with the effects of selected working conditions of face milling, e.g. cutting speed, feed, cutting environment, and cutting forces, on the distribution of residual stresses and on the degree of plastic deformation. Additionally, a brief presentation of XRD abilities and potential in the analysis of technologically treated surfaces is put forward. Some advantageous characteristics of XRD such as lack of limitations due to shape or mechanical properties as hardness of mechanical components are accentuated as well. XRD tensometric methods can supply further detail material structure parameters like qualitative and quantitative presence of crystallographic phases and preferred orientation, i.e. texture which could be created on the analysed surface due to technological processes.

➔ Keywords: Residual stresses, X-ray diffraction, Milling

1 Introduction

There exist several secular trends in machining technologies and one of them it to manufacture a product with highest possible quality and longest possible service life. The quality can be assessed from several points of view, but two main persist. Firstly, the safety is essential for any product usage as it goes hand in hand with reliability. Secondly, producers are being addressed by increasingly sophisticated requests from their customers and hence almost tailor made products are produced which requires not only skilled workforce, but also careful choice of manufacturing technologies. Although milling is counted to traditional machining, it is still frequently used. Quality of milled surface is most commonly considered by roughness, hardness and microhardness. In the last 20 years, some other parameters are being analysed in order to obtain detailed information about surface structure and properties. State of residual stress (RS) represents one of these parameters. So far, it is known that these stresses can be beneficial and increase the fatigue limit in the case of compressive surface stress, but they can have a negative effect, e.g. decreasing the stress corrosion resistance of a material with tensile residual stresses [1, 2]. Working conditions have appreciable impact on creation and/or redistribution of residual stresses in the work-piece. This contribution aims at finding relationship between machining conditions and the resulting state of residual stress [3, 4].

1.1 Influence of cutting speed and feed rate

The aim of the diffraction investigations was to ascertain to what extent the resulting state of residual stresses is influenced by cutting speed and feed rate of face milling process of a surface consisting of steel and cast iron. The specimens' surfaces were measured in several areas in order to detect possible occurrence of surface RS inhomogenities caused mainly by cutting process instabilities. The RS were measured not only on the surfaces, but their depth gradients were obtained as well.

1.1.1 Samples under investigation

The effect of feed rate and cutting speed on RS in machined surfaced layer of guide gibs was studied on the milled steel of Czech grade 14 100.4 (58 – 61 HRC) at seven different cutting conditions. Samples of dimensions 70×30×7 mm³ were cut from machine shears of cast iron 42 2425 (180 – 230 HB) after milling (Fig. 1). All the working and cutting conditions are outlined in Table 1.

XRD analysis of the surface stresses was realised on two chosen areas P1 and P2 (Fig. 2) of 5×5 mm² both in the direction of the cutting tool feed (σ_L) and in the perpendicular direction (σ_T).

The analysis of depth profile of macroscopic residual stress was made only in the centre (area P1) of examined samples.



Fig. 1 Segment of a machine guide gib
Obr. 1 Segment vedení obráběcího stroje

Tab. 1 Working and cutting conditions used in the experiments

Tab. 1 Pracovní a řezné podmínky použité během experimentu

Sample	1	2	3	4	5	6
Cutting operation	parallel milling					
Cutter head	F2254-1000097 Ø160					
Tool diameter [mm]	Ø160					
Tool tips	P3400-100345R 2143					
Number of teeth [-]	24					
Axial depth a_p [mm]	2 x 0,5					
Feed rate [mm/min]	400	300	200	400	400	400
Speed [rpm/min]	120	120	120	150	200	250
Feed per tooth [mm]	0,14	0,10	0,07	0,11	0,08	0,07
Cutting speed [m/min]	60	60	60	75	100	126

1.1.2 Experimental

The measurements were performed on a θ/θ goniometer *X'Pert PRO* with $\text{CrK}\alpha$ radiation. The diffraction line $\{211\}$ of α -Fe phase was analysed. The $\sin^2\psi$ method [5] with eight different tilt angles ψ was used. The X-ray elastic constants $\frac{1}{2}s_2 = 5.76 \cdot 10^{-6} \text{ MPa}^{-1}$, $-s_7 = 1.25 \cdot 10^{-6} \text{ MPa}^{-1}$ were used in macroscopic stress calculations.

Due to the limitations of X-ray penetration depth, the XRD technique can be used only for surface layers few micrometers in thickness. In the case of conventional XRD equipment, investigation of stress depth profiles is performed in combination with electrochemical etching. The process of anodic dissolution takes place during electrochemical etching while the anode is formed by the sample itself; the product of this process is a solution of high electrical resistance which is embedded into microscopic wells in the surface of the sample and, therefore, preferential removal of roughness proceeds [6]. The *LectroPol-5* by *Struers*, a device for automatic micro-processor controlled electrolytic polishing and etching of metallographic specimen was used for surface layer removal.

1.1.3 Results and their discussion

The results of XRD analysis of macroscopic residual stresses from areas P1 and P2 obtained from the surface as well as the average value of the width of the $\{211\}$ diffraction line, which could be interpreted as a degree of plastic deformation of the crystal lattice, are shown in Table 2. Average values of residual stresses and width of diffraction line from areas P1 and P2 are illustrated in Figs. 3–6.

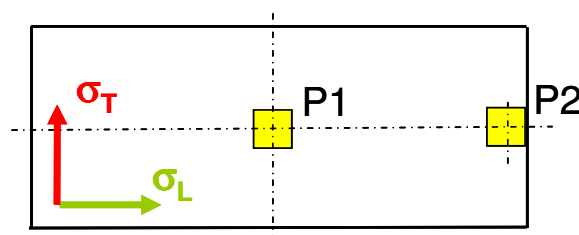


Fig.2 Scheme of the measured surface on samples with marked directions of stress determination σ_L , σ_T and the measured areas P1 and P2

Obr. 2 Schéma měřeného povrchu vzorku s vyznačenými směry měření zbytkových napětí σ_L , σ_T a označenými analyzovanými oblastmi P1 a P2

Tab. 2 Macroscopic residual stresses in longitudinal (σ_L) and transversal (σ_T) directions and the average value of width of the {211} diffraction line obtained from areas P1 and P2

Tab. 2 Makroskopická zbytková napětí ve směru posuvu obráběcího nástroje (σ_L) a ve směru k němu kolmém (σ_T), W reprezentuje průměrnou šířku difrakční linie {211} z analyzovaných oblastí P1 a P2

Sample	Area P1		Area P2		W, deg
	σ_L , MPa	σ_T , MPa	σ_L , MPa	σ_T , MPa	
1	-317	-488	-431	-550	4.74
2	-486	-502	-542	-553	4.90
3	-127	-323	-158	-314	4.12
4	-339	-371	-445	-323	4.84
5	-332	-423	-372	-387	4.92
6	-240	-388	-200	-398	4.71

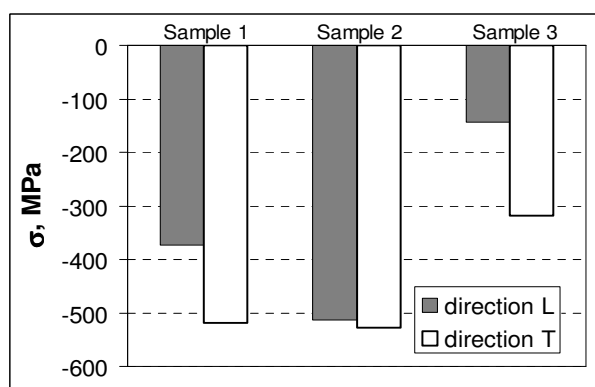


Fig. 3 Average values from areas P1 and P2 of residual stresses σ_L and σ_T from the surface; relation of residual stresses on the feed rate modification

Obr. 3 Průměrné hodnoty povrchových zbytkových napětí σ_L a σ_T z oblastí P1 a P2 v závislosti na posuvu nástroje

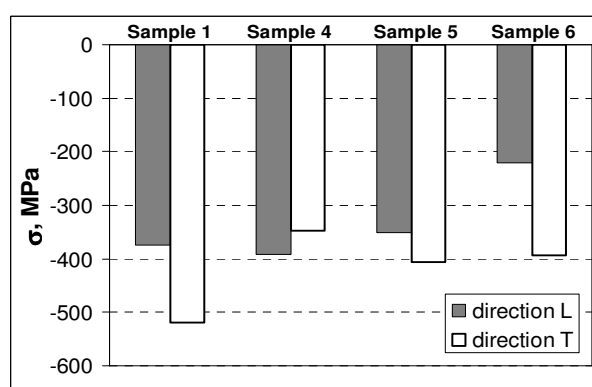


Fig. 4 Average values from areas P1 and P2 of residual stresses σ_L and σ_T from the surface; relation of residual stresses on the cutting speed modification

Obr. 4 Průměrné hodnoty povrchových zbytkových napětí σ_L a σ_T z oblastí P1 a P2 získané v závislosti na řezné rychlosti

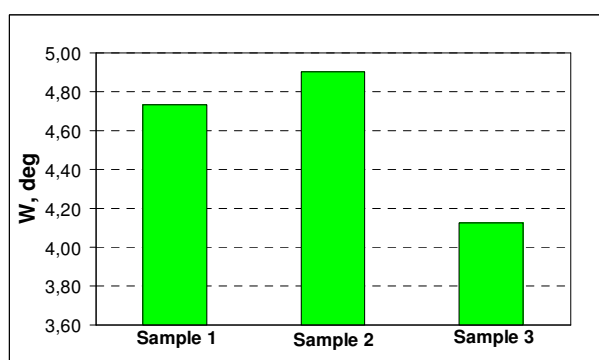


Fig. 5 Average values of width of the {211} diffraction line obtained from areas P1 and P2 from the surface; relation of residual stresses on the feed modification

Obr. 5 Průměrné hodnoty šířky difrakční linie {211} získané z oblastí P1 a P2 analýzy povrchu; závislost na posuvu nástroje

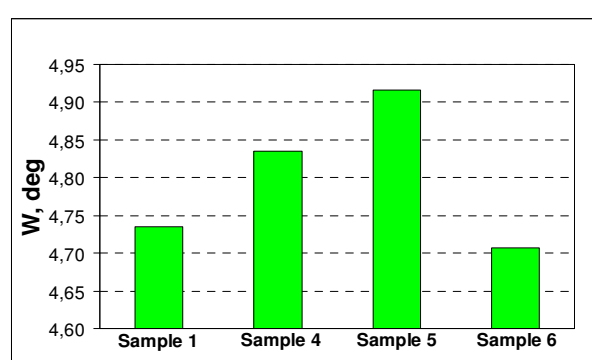


Fig. 6 Average values of width of the {211} diffraction line obtained from areas P1 and P2 from the surface; relation of residual stresses on the cutting speed

Obr. 6 Průměrné hodnoty šířky difrakční linie {211} získané z oblastí P1 a P2, z analýzy povrchu v závislosti na řezné rychlosti

The results of XRD analysis of macroscopic residual stresses from area P1 obtained after gradual etching of the surface as well as the average value of width of the {211} diffraction line are illustrated in Figs. 7 – 12.

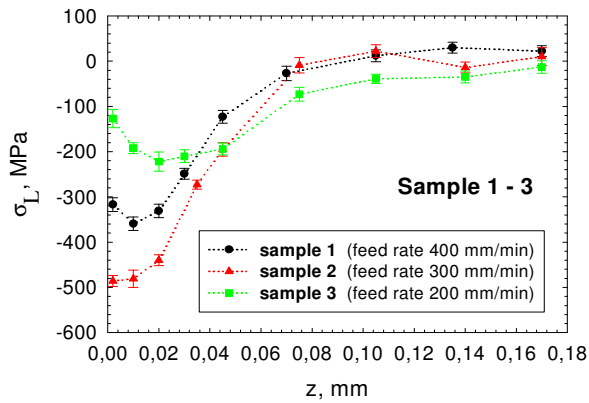


Fig. 7 Depth distribution of residual stresses σ_L obtained for samples 1, 2, and 3
Obr. 7 Průběhy zbytkových napětí σ_L stanovené na vzorcích 1, 2 a 3

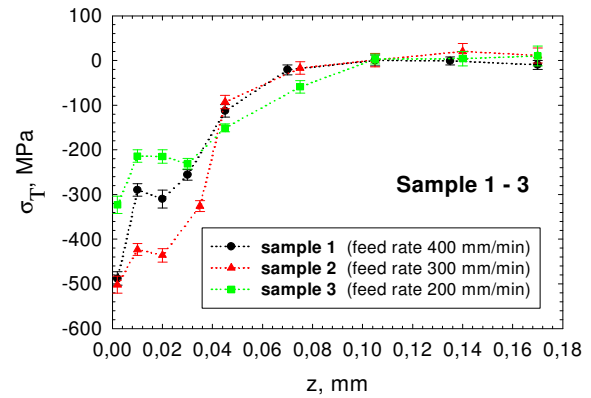


Fig. 8 Depth distribution of residual stresses σ_T obtained for samples 1, 2, and 3
Obr. 8 Průběhy zbytkových napětí σ_T stanovené na vzorcích 1, 2 a 3

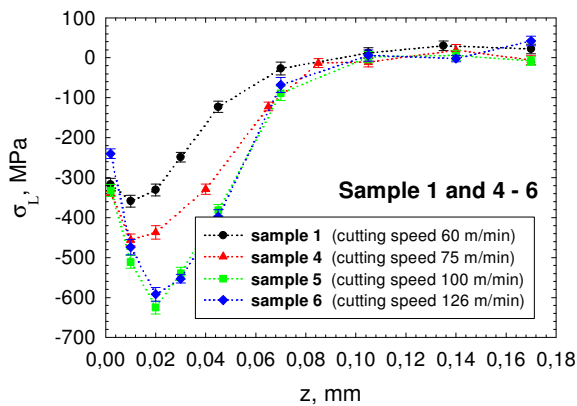


Fig. 9 Depth distribution of residual stresses σ_L obtained for samples 1, 4, 5 and 6
Obr. 9 Průběhy zbytkových napětí σ_L stanovené na vzorcích 1, 4, 5 a 6

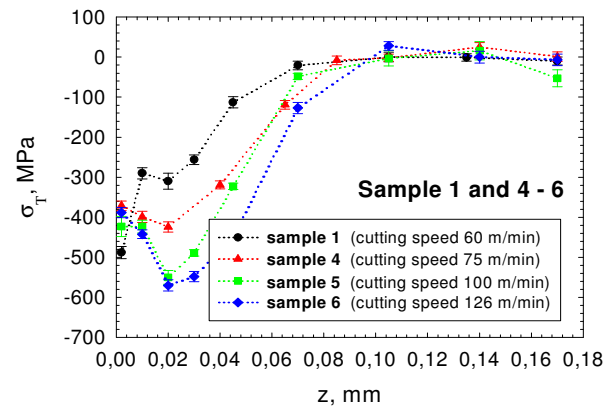


Fig. 10 Depth distribution of residual stresses σ_T obtained for samples 1, 4, 5 and 6
Obr. 10 Průběhy zbytkových napětí σ_T stanovené ze vzorcích 1, 4, 5 a 6

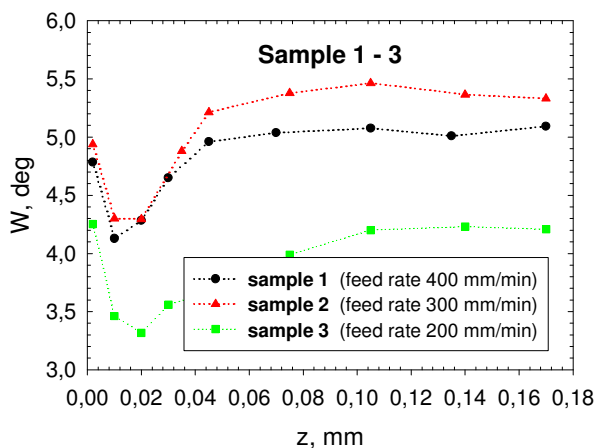


Fig. 11 Average width of the $\{211\}$ diffraction line obtained for samples 1, 2, and 3
Obr. 11 Průměrná šířka difrakční linie $\{211\}$ stanovená na vzorcích 1, 2 a 3

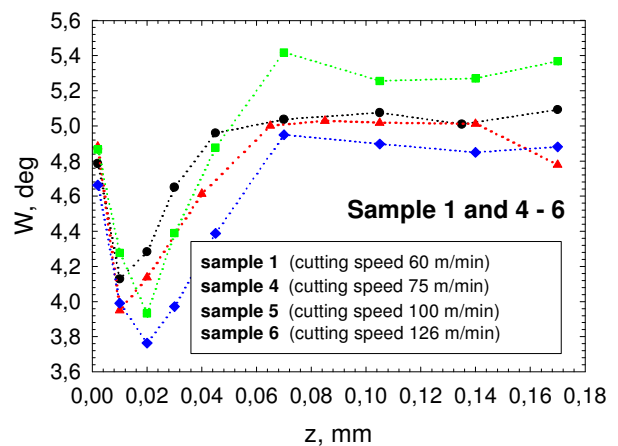


Fig. 12 Average width of the $\{211\}$ diffraction line obtained for samples 1, 2, and 3
Obr. 12 Průměrná šířka difrakční linie $\{211\}$ stanovená na vzorcích 1, 4, 5 a 3

Realised XRD analysis in areas P1 and P2 enables

1. to consider distribution inhomogeneity of residual stresses on the machined surface which results from the instability of cutting process, i.e. mechanical interaction of the cutting tool accompanied with local heating workpiece,
2. to evaluate influence of cutting tool feed during constant cutting speed and effect of cutting speed during constant feed on surface residual stresses and their gradients.

1.1.3.1 XRD analysis of the investigated surfaces

- Favourable compressive residual stresses are observed on the examined surfaces in both directions σ_L and σ_T .
- Samples 1, 2, and 6 show differences in residual stress values in areas P1 and P2. In the case of the sample 1, the difference exceeds 110 MPa and 60 MPa in the direction of tool feed and in the direction of σ_T respectively. The samples 2 and 6 can be characterized by difference of approximately 50 MPa in both the directions.

Effect of tool feed on the distribution of residual stresses

- Average absolute values of residual compressive RS measured in areas P1 and P2 are lower in the direction of tool feed compared with the perpendicular direction (Fig. 3).
- Lower feed rate leads to decrease of differences in residual stress values measured in both selected areas P1 and P2 (Tab. 2), i.e. the stress homogenization occurs with lowering the feed rate.
- Average absolute values of residual stresses and width of the {211} α -Fe diffraction line widths reach maximum for the feed rate of 300 m/min and minimum for feed rate of 200 m/min (Figs. 3 - 5).

Effect of cutting speed on the distribution of residual stresses

- Average absolute values of residual compressive RS in areas P1 and P2 measured for samples 1, 5, 6 (Fig. 4) are always lower in the tool feed direction, the only exception is the sample 4.
- Widths of {211} α -Fe diffraction line increase with rising cutting speed, but the sample 6 machined by using the highest cutting speed of 126 m/min contradicts this behaviour since it exhibits the lowest value of diffraction line width and hence the lowest degree of plastic deformation. This effect is probably caused by differences in temperature fields in the cutting zone for the used cutting speeds which has appreciable impact on the cutting forces.

1.1.3.2 Gradients of residual stresses

- Favourable compressive residual stresses were observed on the examined samples and, in the majority of samples, the hook-like depth distributions of macroscopic residual stresses were recorded. Distributions of σ_L and σ_T in samples 1, 2, and 3 prove that change in feed rate results in the change of distribution profiles, yet the affected zones remain the same, reaching approximately 80 μm (Figs. 7 & 8).
- Profiles of depth distributions σ_L and σ_T are qualitatively different.
- Samples 1, 2, and 3 exhibit anisotropic state of macroscopic residual stress ($\sigma_L \neq \sigma_T$) which becomes isotropic ($\sigma_L \approx \sigma_T$) in depths deeper than 0.02 mm. This effect is probably caused by the nature of mechanical interaction of cutting tool with the work-piece, type of tool tips and working conditions.
- The zone affected by machining is the same for all applied cutting speeds (Figs. 9 and 10) and its value reaches typically 80 μm .
- The effect of cutting speed is pronounced on sub-surface values of residual stresses σ_L and σ_T . The absolute values of residual compressive RS rise in both investigated directions with rising cutting speed till the threshold of 100 m/min. Further acceleration of milling process to 126 m/min has analogous consequence only for σ_T (Fig. 10); the stress gradient of σ_L barely changes in this case (Fig. 9)

1.2 Influence of cutting forces

The goal of this investigation was to establish a relationship between cutting forces during face milling on the resulting distribution of RS. Six different cooling environments were applied during the machining process.

1.2.1 Samples under investigation

A set of experimental samples was subjected to face milling with cutting head diameter of 80 mm and with five tool tips *SPEW 1204ADSN*. The cutting conditions were the same for all samples, i.e. depth of cut 1 mm, feed rate 1.5 meters per rotation and cutting speed of 135 meters per minute, the only difference being the lubricant and coolant. Four various liquid lubricants were used, namely *Microcool 387+*, *Paramo SK 300*, *Accu-Lube LBB 2000*, *Solgreen 540*. One sample was milled using cooled air of 4 °C from a Ranque-Hilsch vortex tube and one sample just on the ambient air. The coolant *Accu-Lube LBB 2000* was applied in the form of mist, or the so-called *MQL*

A tough material – mild carbon steel – was chosen for samples' manufacturing. The dimensions of cuboid-shaped samples were 70×15×50 mm³ and the selected face that underwent milling is depicted in Fig. 13.

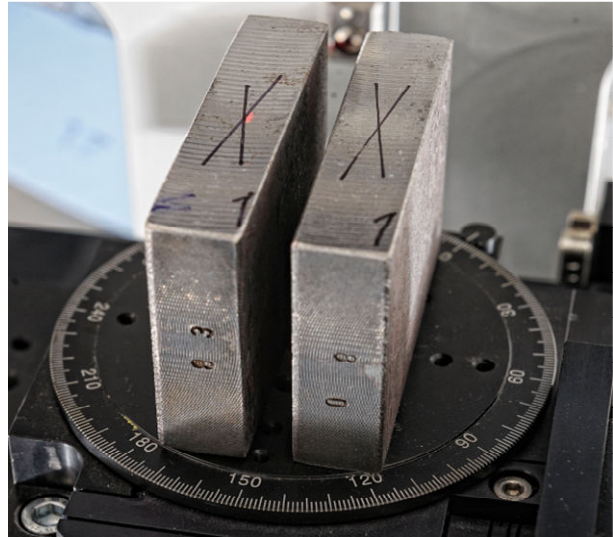


Fig. 13 Experimental samples placed on a set of x, y, z translation and rotation stages. The measured surfaces are marked with cross
Obr. 13 Experimentální vzorky umístěné na translačním a rotačním stolku jenž umožňuje přesné nastavení analyzovaného místa

1.2.2 Experimental

Machining forces were measured in a traditional yet reliable way, i.e. by *Kistler* dynamometer which was placed under a holder with a machined sample. The dynamometer enables to obtain F_f – force in the feed direction, F_p – force in the direction of in-feed motion, F_c – cutting force. The forces began to be measured after the threshold of 30 N was breached and lasted for 2 seconds during which 2000 values were recorded. Typical example of such force evolution is shown in Fig. 14. The values characterizing F_f , F_c , and F_p were evaluated as mean values of the last 500 local maximums corresponding to each of the three measured magnitudes.

The tensometry analysis was carried out in the same manner as in the case of investigation in the chapter 1.1.

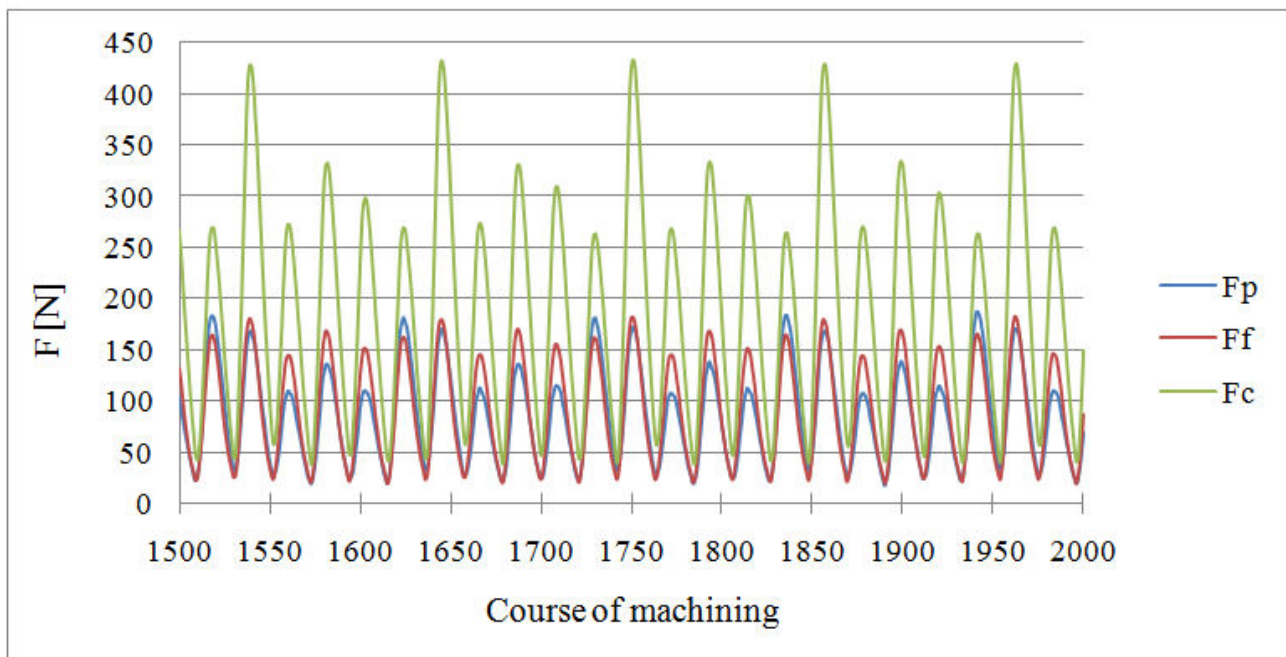


Fig. 14 Example of a record of milling forces measurement
Obr. 14 Příklad záznamu měření řezných sil v průběhu experimentu

1.2.3 Results and their discussion

All the analyzed magnitudes are briefly summarized in Tab. 2 in order to provide clear and straightforward preview revealing any mutual relationships.

Tab. 2 Mean values of measured forces, macroscopic RS in the feed direction (σ_L), perpendicular to feed direction (σ_T) and {211} peak width (FWHM) for $\psi = 0^\circ$

Tab. 2 Hodnoty řezných sil, makroskopická zbytkových napětí ve směru posuvu nástroje σ_L a ve směru k němu kolmém (σ_T) a střední šířka W difrakční linie {211} při $\psi = 0^\circ$

	F_p , N	F_C , N	F_f , N	σ_L , MPa	σ_T , MPa	W , deg
air	381	413	296	258 ± 12	325 ± 31	2.617
air 4 °C	328	421	274	280 ± 18	401 ± 25	2.708
MQL	288	357	209	314 ± 12	551 ± 64	2.818
Microcool 387+	229	355	216	488 ± 20	575 ± 66	2.892
Solgreen 540	220	352	195	490 ± 12	303 ± 50	2.696
Paramo SK 300	166	323	168	503 ± 21	518 ± 47	2.781

1.2.3.1 R_m to $R_{p0.2}$ criterion

For tough and plastic metals that characteristically produce continuous chip or a spiral during milling, the ratio of tensile strength R_m to yield strength $R_{p0.2}$ is to be larger than 1.25 [7]. In case of the analyzed mild carbon steel C45 it gives:

$$\frac{R_m}{R_{p0.2}} = \frac{620 \text{ MPa}}{340 \text{ MPa}} = 1.82 > 1.25$$

And therefore during the formation of the continuous chip, surface is being stretched out and tensile residual stresses are expected to be generated on the surface and sub-surface areas.

1.2.3.2 XRD analysis of the investigated surfaces

- All the analyzed surfaces exhibit tensile normal macroscopic RS σ_L & σ_T . This is coincordance with our expectations considering the toughness of the machined material.
- The lowest values of σ_L were found for dry milling. In these cases no lubricant was present on the machined zone.
- The sample milled with presence of liquid with the lowest measured forces in the in-feed direction sticks out by the highest tensile RS in the feed direction.
- There exists a clearly visible correlation: with decreasing cutting forces in both the feed and in-feed direction, the RS in the feed direction increases.

2 XRD method as an ideal tool for diagnostic of surfaces after manufacturing technologies

Diffraction analysis of residual stresses can be counted among the most elaborate tensometric method. Over the last two decades, it has gained more attention and popularity due to the marked improvements in diffractometry techniques and experimental devices. It also requires skilled operating personnel with vast knowledge in physics, mathematics and at least decent degree of dexterousness. In a contrast to other techniques, this also furnishes data about reliability of the obtained values, i.e. standard deviations and confidence intervals. Moreover, it serves as a convenient tool for depth distribution studies when performed in combination with electro-chemical etching. XRD is not limited by the shape and some mechanical properties such as high hardness. The scope of gainable information from XRD measurements is listed in the following:

- Complete tensor of macroscopic RS is obtained; the RS could be measured in each present crystalline phase; microscopic RS can be calculated which is especially beneficial as it often correlates with microhardness.
- Diffraction profile analysis can yield results having close relationship to the degree of plastic deformation during the surface creation processes.

- Influence of bending and torsion on the material structure can be online monitored.
- Homogeneity of the surface can be monitored in detail; the investigated area, i.e. the domain irradiated by primary X-ray beam, can be as small as 1 mm².
- RS in thin layers with thickness from 100 nm can be determined.
- Qualitative and quantitative phase composition can be established with 1% accuracy.
- Temperature dependent phase transformation can be monitored in situ up to 2300 °C.
- Preferred orientation of grains in polycrystalline material, or the so called texture, can be measured; this is of special significance in some manufacturing processes such as rolling etc.

3 Conclusions

Two examples of XRD tensometry analysis performed in the XRD laboratory of Faculty of nuclear sciences and physical engineering of CTU in Prague are presented in this contribution. Their aim was to establish the state of macroscopic residual stress and the degree of plastic deformation in the face milled surface layers.

XRD tensometry is a rapidly growing technique which is gaining attention not only at academic spheres, but also in industry. All over the world, several government and private laboratories has been founded. They offer service and consultancy to a wide and diverse group of customers. Hence, another goal was to offer a brief list of XRD capabilities which would be of special use for technologist and personnel of technological laboratories, designer from various industrial fields and staff from technical universities.

It is generally acknowledged that the majority of machine components failures are caused by the fatigue of material often initiated by cyclic loading. It has been shown that, in general, compressive RS in the material can favourably reinforce the dynamic strength by about 50 per cent; on the other hand, tensile RS could reduce the dynamic strength by about 30 per cent. Together with the phase transformations, RS form an important factor affecting the failure. Moreover, assiduous analyses of such failures have furnished sufficient evidence that local properties of the most severely loaded zone, which is often the surface, are crucial.

The sensitivity of fatigue limit is most pronounced on the surface and it depends on the locally changed properties of the surface layer after a technological treatment. Such surface is also distinguished by the elevated probability of deformed grains, vacancies, and dislocations, which had come to life as a result of plastic deformation and thermal fields present during manufacturing. In this respects, XRD tensometry is an optimal analytic technique for surface structure and surface properties analysis.

Acknowledgements

The research was supported by the Project No 101/09/0702 of the Czech Science Foundation and by the Project MSM 6840770021 of the Ministry of Education, Youth and Sports of the Czech Republic.

References

- 1 Jeelani S. and Musial M. Effect of cutting speed and tool rake angle on the fatigue life of 2024-T351 aluminum alloy, *International Journal of Fatigue*, 6(3), pp. 169–172 (1984). ISSN 0142-1123.
- 2 Sasahara H. The effect on fatigue life of residual stress and surface hardness resulting from different cutting conditions of 0.45%C steel, *International Journal of Machine Tools and Manufacture*, 45(2), pp. 131-136 (2005). ISSN 0890-6955.
- 3 Sridhar B.R., Devananda G., Ramachandra K. and Bhat R. Effect of machining parameters and heat treatment on the residual stress distribution in titanium alloy IMI-834, *Journal of Materials Processing Technology*, 139(1-3), pp. 628-634 (2003). ISSN 0924-0136.
- 4 Bouzid Saï W., Ben Salaha N. and Lebrunb J.L. Influence of machining by finishing milling on surface characteristics, *International Journal of Machine Tools and Manufacture*, 41(3), pp. 443-450 (2001). ISSN 0890-6955.
- 5 Kraus I. and Ganey N. *Technické aplikace difrakční analýzy*, (ČVUT, Praha, 2004). ISBN 80-01-03099-7.

- 6 Lee S. J., Lee Y. M. and Du M. The polishing mechanism of electrochemical mechanical polishing technology, *Journal of Materials Processing Technology*, 140(1-3), pp. 280-286 (2003). ISSN 0924-0136.1.
- 7 NECKÁŘ, F. – KVASNIČKA, I. *Vybrané statě z úběru materiálu*. 1 vyd., Praha : ČVUT, 1991. 88 s. ISBN 80-01-00696-4.

Difrakční analýza zbytkových napětí třískově obrobených ploch

Ing. Kamil Kolařík, Ph.D.¹, prof. Ing. Nikolaj Ganev, CSc.², Ing. Zdenek Pala¹,
Doc. Ing. Jan Jersák, CSc.²

¹ Katedra inženýrství pevných látek, Fakulta jaderná a fyzikálně inženýrská, ČVUT v Praze, Trojanova 13, 120 00 Praha 2, ČR

² Katedra obrábění a montáže, Fakulta strojní, TUL v Liberci, Studentská 2, 461 17 Liberec 1, ČR

➔ Klíčová slova: zbytková napětí, rentgenová difrakce, frézování

Interakce řezného nástroje s materiálem v průběhu opracování se realizuje přes jeho volný povrch, a proto může stav povrchových vrstev ovlivnit rozhodujícím způsobem užitkové vlastnosti celého objemu. Jedním z nejvýznamnějších faktorů, který musí být v této souvislosti uvažován, je redistribuce zbytkových napětí doprovázejících každý technologický proces, při němž dochází k nehomogenní plastické a tepelné deformaci.

Analýza zbytkových napětí má při diagnostice užitných vlastností strojních dynamicky namáhaných komponent stále rostoucí význam a vhodně doplňuje klasické materiálové charakteristiky (pevnost, houževnatost, otěruvzdornost).

V prezentovaném příspěvku jsou uvedeny dva příklady aplikací rtg difrakční tenzometrické analýzy v laboratoři strukturní rentgenografie Fakulty jaderné a fyzikálně inženýrské ČVUT v Praze při studiu vlivu vybraných parametrů pracovních podmínek (např. řezná rychlost, posuv nástroje, řezné prostředí a síly při obrábění) na rozložení zbytkových napětí a míru plastické deformace v povrchových vrstvách po čelním frézování.

Dalším cílem předkládaného příspěvku je stručná prezentace možností rtg difrakce při studiu technologicky opracovaných povrchů, kdy difrakční techniky nejsou omezené tvarem a mechanickými vlastnostmi (např. tvrdostí) strojních komponent, jako je tomu u jiných tenzometrických metod. Rentgenografické metody mohou navíc poskytovat informace o přítomnosti a zastoupení jednotlivých fází a textuře – přednostní orientaci zrn, vznikající na analyzované ploše v důsledku technologického opracování.

